Bias-modulated dynamics of a strongly driven two-level system

Zhiguo Lü,[1,2,*] Yiying Yan,[1,2] Hsi-Sheng Goan,[3,4,†] and Hang Zheng[1,2,‡]

[1]*Key Laboratory of Artificial Structures and Quantum Control (Ministry of Education), Department of Physics and Astronomy, Shanghai Jiao Tong University, Shanghai 200240, China*

[2]*Innovation Center of Advanced Microstructures, Nanjing 210093, China*

[3]*Department of Physics and Center for Theoretical Sciences, National Taiwan University, Taipei 10617, Taiwan*

[4]*Center for Quantum Science and Engineering, National Taiwan University, Taipei 10617, Taiwan*

(Received 27 October 2015; published 2 March 2016)

We investigate the bias-modulated dynamics of a strongly driven two-level system using the counterrotating-hybridized rotating-wave (CHRW) method. This CHRW method treats the driving field and the bias on equal footing by a unitary transformation with two parameters ξ and ζ, and is nonperturbative in driving strength, tunneling amplitude, or bias. In addition, this CHRW method is beyond the traditional rotating-wave approximation (Rabi-RWA) and yet by properly choosing the two parameters ξ and ζ, the transformed Hamiltonian takes the RWA form with a renormalized energy splitting and a renormalized driving strength. The reformulated CHRW method possesses the same mathematical simplicity as the Rabi-RWA approach and thus allows us to calculate analytically the dynamics and explore explicitly the effect of the bias. We show that the CHRW method gives the accurate driven dynamics for a wide range of parameters as compared to the numerically exact results. When energy scales of the driving are comparable to the intrinsic energy scale of the two-level systems, the counterrotating interactions and static bias profoundly influence the generalized Rabi frequency. In this regime, where ordinary perturbation approaches fail, the CHRW works very well and efficiently. We also demonstrate the dynamics of the system in the strong-driving and off-resonance cases for which the Rabi-RWA method breaks down but the CHRW method remains valid. We obtain analytical expressions for the generalized Rabi frequency and bias-modulated Bloch-Siegert shift as functions of the bias, tunneling, and driving field parameters. The CHRW approach is a mathematically simple and physically clear method. It can be applied to treat some complicated problems for which a numerical study is difficult to perform.

DOI: 10.1103/PhysRevA.93.033803

I. INTRODUCTION

Quantum mechanically two-level systems (TLSs) provide an ideal testing ground for exploring nonclassical phenomena and understanding the nature of quantum physics [1,2]. The primary importance of a TLS in the fast developing area of quantum information processing is in its controlled manipulation as the elementary building block, called a qubit [3]. The controllable dynamics of a driven TLS is at the core of many vastly different state-of-the-art technologies, especially solid-state implementations of individually addressable TLSs [4]. The studies of driven TLSs have quite a rich history, and wide application for both experimental and theoretical investigations [5–15]. Recently, great progress has been made experimentally using superconducting devices based on Josephson tunnel junctions [16–21], optically and electrically controlled single spins in quantum dots [22–26], individual charge in quantum dots [27,28], and nitrogen vacancy center in diamond [29–31], for the implementation of the controllable coherent dynamics of qubits.

Periodically time-dependent driving fields are widely employed to realize the control and manipulations of qubits. The prototype here described by the semiclassical Rabi model in the tunneling or localized representation is

$$H(t) = -\frac{\Delta}{2}\sigma_x - \frac{\varepsilon(t)}{2}\sigma_z = -\frac{\Delta}{2}\sigma_x - \left(\frac{\epsilon}{2}\sigma_z + \frac{A\cos(\omega t)}{2}\sigma_z\right), \tag{1}$$

where Δ is a time-independent tunneling strength, $\varepsilon(t)$ is a driving field with a static bias ϵ, $A\cos(\omega t)$ is a periodical driving field with amplitude A and frequency ω, and the symbols σ_x, σ_y, and σ_z are the usual Pauli matrices. We set throughout this paper $\hbar = 1$. Subjecting the Hamiltonian to a rotation about the y axis, we get a new representation $\exp(i\pi\sigma_y/4)H(t)\exp(-i\pi\sigma_y/4) = -\frac{\Delta}{2}\sigma_z + \frac{\varepsilon(t)}{2}\sigma_x$. This is the Hamiltonian typically used in quantum optics and nuclear magnetic resonance in which Δ is energy difference between the two levels and the driving term is responsible for the transitions between them.

The Hamiltonian of Eq. (1) can represent, for example, a flux qubit with a static bias and a driving field in the persistent current basis. Although this Hamiltonian looks simple, there exist a wide variety of interesting dynamical features [32], such as Rabi oscillations, the invalidity of the RWA [33], Bloch-Siegert shifts [6,34,35], nonlinear phenomena due to level crossings induced quantum interference, coherent destruction of tunneling (CDT), and the possibility of chaos [36–39]. Thus, even for this simplest driven TLS model with a sinusoidal driving field $A\cos(\omega t)$, it is a difficult task to present an analytical and exact solution transparently. In order

*zglv@sjtu.edu.cn
†goan@phys.ntu.edu.tw
‡hzheng@sjtu.edu.cn

to discover the driven tunneling physics analytically, a number of approximate methods, such as Rabi-RWA and the RWA in a rotating frame (RWA-RF) of Refs. [33,40], have been developed, even though the dynamics of the Rabi model can be solved exactly by numerical methods. We discuss briefly the conditions to make the Rabi-RWA for the Hamiltonian of Eq. (1) and the dynamics of the driven TLS using the Rabi-RWA method in the Appendix.

It is interesting and important to study how the counter-rotating (CR) terms and static bias together influence the dynamics in a wide range of parameter space, especially in the regime where the relevant energy scales are of the same order, i.e., $\epsilon \sim \Delta \sim A \sim \omega$. When the energy scales are near the same, the perturbation based on Δ, A, or ϵ becomes invalid. Therefore, it is necessary to develop an alternative analytical method to extract the physics in this specific parameter regime. Moreover, only for the zero-bias case and when the CR terms are dropped (in other words, the Rabi-RWA method is applicable), can the dynamics of Eq. (1) be solved analytically. For the finite bias case, the Rabi-RWA Hamiltonian reduced from the Hamiltonian of Eq. (1) by neglecting all the fast oscillatory terms in the energy eigenbasis can then be analytically solvable. This raises the question on the validity of the results in the strong driving strength and off-resonance ($\omega \neq \Xi_0 = \sqrt{\Delta^2 + \epsilon^2}$) regimes where the breakdown of the reduced Rabi-RWA Hamiltonian occurs [6]. Recently, it has been found that the effects of CR terms are significant in different interesting topics, such as quantum Zeno effect [41], entanglement evolution [42], resonance fluorescence [43], and so on. On the other hand, in the context of superconducting flux qubits, recent investigations of strong driving-induced effects on Rabi oscillations [35,44] prompt us to investigate the problem of how much the Rabi frequency and Bloch-Siegert shift would change as a function of the static bias ϵ.

The main purpose of this paper is to demonstrate the significant role of the bias and the driving on the time evolution and physical properties of the driven TLS. The dynamics of the TLS with far off-resonance and strong driving strength conditions is interesting but difficult to study analytically due to its complexities [32,40]. The availability of accurate and transparent analytic evaluation of the dynamics is very useful and important. In our previous papers [45,46], we proposed the counterrotating-hybridized rotating-wave (CHRW) method to analytically treat the driven dynamics and numerically calculate Bloch-Siegert shift at zero bias. In the present paper, we develop a novel analytical method using the idea of CHRW to systematically study finite bias cases, which are realistically operated in current experiments. The major difference from our previous papers and the main result of the current paper are as follows. (i) From the viewpoint of methodology, in order to take into account the resultant effects of static bias, our present approach adopts a unitary transformation with a two-parameter (ξ and ζ) generator of Eq. (2) in contrast with a simple unitary transformation with a single parameter ξ for the unbiased case in our previous papers [45,46]. The present developed CHRW approach paves a way to investigate the physics of the bias in a driven TLS. (ii) The bias ϵ modulates the energy levels of the TLS and therefore modulates the resonant condition between a driving field and the TLS. It is interesting and important to investigate the effects of bias on the dynamics of the TLS and the competition between the bias and driving. In broad regions of the ϵ-extended parameter space (near resonance $\Xi_0 \sim \omega$ and off-resonance $\Xi_0 < \omega$), we find that our CHRW results are in very good agreement with the exact numerical results. We demonstrate the significant role of the CR coupling and the bias on the time evolution and physical properties of the driven TLS. (iii) We calculate the generalized Rabi frequency and the bias-modulated Bloch-Siegert shift that can be measured in experiments [35,44]. Our results are in good agreement with those of the flux qubit data presented in Ref. [44]. (iv) After comparing the results obtained by our method with those of the other RWA methods, the second-order Van Vleck (2nd-VV) perturbation method and the exact numerical method, we demonstrate the various parameter regimes for the validity of the different methods and show clearly that our CHRW method is more efficient and accurate than the other RWA and perturbation methods we discuss.

As the Hamiltonian Eq. (1) can be numerically solved easily and quickly by the Floquet theory, why do we pursue an approximate analytical solution? The reasons are as follows. A good approximate analytical solution should be as simple as possible, especially mathematically, so that it can be straightforwardly extended to investigate more complicated situations where a numerical study is hard to perform. More importantly, the main physics should be described pretty well and the dynamics should be as accurate as possible when compared with the numerically exact results, at least for the interesting and concerned range of the parameters (especially those of experimental relevant parameter regimes). The simple analytical CHRW method we provide does have such merits. The CHRW method is beyond the Rabi-RWA and enables one to understand the physics, such as effects of the CR coupling and the bias, more clearly. The important physical properties in the driven system, such as the generalized Rabi frequencies and Bloch-Siegert shifts, which are not easy to extract directly from the time evolution by the numerical methods, can be calculated in analytical forms. Our CHRW method can also explore explicitly important physical phenomena, for example, the CDT, and describe other important dynamical features and behaviors very well for a wide range of parameters. Furthermore, it can be applied to other more complicated models or driven open quantum systems where numerically exact solutions are hard to obtain. Besides, it is interesting to discuss the validity of different RWA schemes and show how the previous results appear in the various limits of the CHRW method.

The structure of this article is as follows. In Sec. I, we introduce the driving TLS model with a static bias. In Sec. II, we develop a simple and efficient method to analytically and quantitatively solve the monochromatically driven dynamics. In Sec. III, we analyze the dynamics in a wide parameter regime including the cases of resonance, near resonance, and far-off resonance. Moreover, we demonstrate in Sec. IV the effects of the CR wave terms and the bias on the dynamics, the generalized Rabi frequency, and the Bloch-Siegert shift. Finally, we give the parameter regions for the CHRW method to be valid before we present a short conclusion in Sec. V.

II. COUNTERROTATING-HYBRIDIZED ROTATING-WAVE METHOD

In this section, we describe the CHRW method to calculate the driven tunneling dynamics for the finite bias case [45–47]. In the CHRW method a time-dependent unitary transformation $\exp(S)$ is applied to the system and we propose the generator of the unitary transformation to be

$$S = -i\frac{A}{2\omega}\sin(\omega t)[\xi\sigma_z + \zeta\sigma_x]. \tag{2}$$

The two significant parameters ξ and ζ introduced in S will be determined later on. We use the time-dependent Schrödinger equation $i\frac{d}{dt}|\Psi(t)\rangle = H(t)|\Psi(t)\rangle$ to solve the dynamics. After the unitary transformation, we obtain readily the interaction picture formulas with $|\Psi'(t)\rangle = \exp(S)|\Psi(t)\rangle$ and $i\frac{d}{dt}|\Psi'(t)\rangle = H'(t)|\Psi'(t)\rangle$. Here the transformed Hamiltonian is

$$\begin{aligned} H' = &-\frac{\Delta}{2}\left[\sigma_x - \frac{1-\cos\Theta}{X^2}\xi(\xi\sigma_x - \zeta\sigma_z) + \frac{\sin\Theta}{X}\xi\sigma_y\right] \\ &-\frac{\varepsilon(t)}{2}\left[\sigma_z + \frac{1-\cos\Theta}{X^2}\zeta(\xi\sigma_x - \zeta\sigma_z) - \frac{\sin\Theta}{X}\zeta\sigma_y\right] \\ &+\frac{A}{2}(\xi\sigma_z + \zeta\sigma_x)\cos(\omega t), \end{aligned} \tag{3}$$

where

$$\Theta = \frac{A}{\omega}X\sin(\omega t), \tag{4}$$

$$Z = \frac{A}{\omega}X, \tag{5}$$

$$X = \sqrt{\xi^2 + \zeta^2}. \tag{6}$$

After making use of the relation [33]

$$\exp(iz\sin\alpha) = \sum_{n=-\infty}^{\infty} J_n(z)e^{in\alpha}, \tag{7}$$

where $J_n(z)$ are the nth-order Bessel functions of the first kind, we divide the Hamiltonian into three parts $H' = H'_0 + H'_1 + H'_2$ according to the order of the harmonics (photon transfer process: 0 photon, 1 photon, ..., m photons), where

$$H'_0 = -\frac{\tilde{\Delta}}{2}\sigma_x - \frac{\tilde{\epsilon}}{2}\sigma_z, \tag{8}$$

$$\begin{aligned} H'_1 = &-\frac{(\Delta\xi - \epsilon\zeta)}{X}J_1(Z)\sin(\omega t)\sigma_y \\ &-\frac{A}{2}[1 - \xi - \zeta^2 J_c]\cos(\omega t)\sigma_z \\ &+\frac{A}{2}\zeta[1 - \xi J_c]\cos(\omega t)\sigma_x, \end{aligned} \tag{9}$$

$$\begin{aligned} H'_2 = &\frac{A}{2}\frac{\zeta}{X}J_1(Z)\sin(2\omega t)\sigma_y \\ &-\frac{(\Delta\xi - \epsilon\zeta)}{X^2}J_2(Z)\cos(2\omega t)(\xi\sigma_x - \zeta\sigma_z) \\ &+\frac{A}{2}\frac{\zeta}{X^2}J_2(Z)\cos(3\omega t)(\xi\sigma_x - \zeta\sigma_z) \\ &-\frac{[\Delta\xi - \varepsilon(t)\zeta]}{X^2}\sum_{n=2}^{\infty}\{XJ_{2n-1}(Z)\sin[(2n-1)\omega t]\sigma_y \\ &+J_{2n}(Z)\cos(2n\omega t)(\xi\sigma_x - \zeta\sigma_z)\}, \end{aligned} \tag{10}$$

and the parameters $\tilde{\Delta}$, $\tilde{\epsilon}$ and J_c are defined as

$$\tilde{\Delta} = \Delta - \frac{\xi}{X^2}[1 - J_0(Z)](\Delta\xi - \epsilon\zeta), \tag{11}$$

$$\tilde{\epsilon} = \epsilon + \frac{\zeta}{X^2}[1 - J_0(Z)](\Delta\xi - \epsilon\zeta), \tag{12}$$

$$J_c = \frac{1 - J_0(Z) - J_2(Z)}{X^2}. \tag{13}$$

Note that the zero-ω Hamiltonian H'_0 consists of the renormalized tunneling $\tilde{\Delta}$ and the renormalized bias $\tilde{\epsilon}$, both with a modified factor $J_0(AX/\omega)$ including infinite order of A [see Eqs. (11) and (12)]. H'_1 contains all single-ω terms in the transformed Hamiltonian with a factor $J_1(AX/\omega)$, which relates to single-photon assisted transitions and H'_2 includes all higher-order harmonic terms such as $\cos(n\omega t)$ and $\sin(n\omega t)$ with $n \geqslant 2$.

The Hamiltonian H'_0 can be diagonalized by a unitary matrix $U = u\sigma_z - v\sigma_x$ with

$$u = \sqrt{\frac{1}{2} - \frac{\tilde{\epsilon}}{2\tilde{\Xi}}}, \quad v = \sqrt{\frac{1}{2} + \frac{\tilde{\epsilon}}{2\tilde{\Xi}}}, \tag{14}$$

into the form

$$\tilde{H}_0 = \frac{\tilde{\Xi}}{2}\tau_z, \tag{15}$$

where τ_z is the z-component spin operator in the energy eigenbasis and

$$\tilde{\Xi} = \sqrt{\tilde{\Delta}^2 + \tilde{\epsilon}^2} \tag{16}$$

is the renormalized energy splitting. At the same time H'_1 becomes a little bit complicated $\tilde{H}_1 = U^\dagger H'_1 U$ in the new energy basis,

$$\begin{aligned} \tilde{H}_1 = &\frac{(\Delta\xi - \epsilon\zeta)}{X}J_1(Z)\sin(\omega t)\tau_y \\ &+\frac{A}{2}[1 - \xi - \zeta^2 J_c]\cos(\omega t)\left(\frac{\tilde{\epsilon}}{\tilde{\Xi}}\tau_z + \frac{\tilde{\Delta}}{\tilde{\Xi}}\tau_x\right) \\ &+\frac{A}{2}\zeta[1 - \xi J_c]\cos(\omega t)\left(\frac{\tilde{\epsilon}}{\tilde{\Xi}}\tau_x - \frac{\tilde{\Delta}}{\tilde{\Xi}}\tau_z\right), \end{aligned} \tag{17}$$

where τ_x and τ_y are, respectively, the x-component and the y-component spin operators in the energy eigenbasis. Then, in order to make the driving interaction term $\tilde{H}_1 = U^\dagger H'_1 U$ hold the RWA-like interaction form, we choose the two proper parameters ξ and ζ to satisfy the following two self-consistent conditions. First, we require the coefficient of counterrotating terms $\exp(\pm i\omega t)(\tau_x \pm i\tau_y)/2$ in Eq. (17) to vanish, so we have

$$\begin{aligned} 0 = &\frac{A}{2}\left[\frac{\tilde{\Delta}}{\tilde{\Xi}}[1 - \xi - \zeta^2 J_c] + \frac{\tilde{\epsilon}}{\tilde{\Xi}}\zeta(1 - \xi J_c)\right] \\ &-\frac{\Delta\xi - \epsilon\zeta}{X}J_1(Z). \end{aligned} \tag{18}$$

Second, we require the coefficients of $\frac{A}{2}\cos(\omega t)\tau_z$ term in H_1' to be zero. This then leads to

$$0 = \tilde{\epsilon}(1 - \xi - \zeta^2 J_c) - \tilde{\Delta}\zeta(1 - \xi J_c). \tag{19}$$

The two parameters ξ and ζ can be self-consistently solved by Eqs. (18) and (19). Notice that from Eq. (3) to Eq. (19), no approximation is involved.

In the following treatment, we keep all the zeroth and first harmonics of the transformed driven Hamiltonian ($n\omega$, $n = 0,1$) $\tilde{H}_0 + \tilde{H}_1$ and neglect the higher-order harmonic terms of $\tilde{H}_2 = U^\dagger H_2' U$ that involves all multi-ω or multiphoton assisted transitions ($n\omega$, $n = 2,3,4,\ldots$) in the transformed energy eigenbasis. The validity of the omission of $\tilde{H}_2$ or H_2' depends on the effects of the higher-frequency driving terms ($n \geqslant 2$), i.e., the fast-oscillating term, generally accompanying the second-order or higher-order Bessel functions. Its contribution to the dynamics is not prominent except for the ultrastrong driving-strength case. This is called the CHRW method and we obtain the reformulated RWA Hamiltonian

$$\begin{aligned} H_{\rm CHRW} &= \tilde{H}_0 + \tilde{H}_1 \\ &= \frac{\widetilde{\Xi}}{2}\tau_z + \frac{\tilde{A}}{2}[\tau_+ \exp(-i\omega t) + \tau_- \exp(i\omega t)], \end{aligned} \tag{20}$$

where $\tau_\pm = (\tau_x \pm i\tau_y)/2$, $\widetilde{\Xi}$ is the renormalized energy splitting involved with the static bias's modulation, and $\tilde{A}$ is the renormalized amplitude of the driving field resulting from the combination of the CR coupling and static bias,

$$\tilde{A} = A\left[\frac{\tilde{\Delta}}{\widetilde{\Xi}}(1 - \xi - \zeta^2 J_c) + \frac{\tilde{\epsilon}}{\widetilde{\Xi}}\zeta(1 - \xi J_c)\right] \tag{21}$$

$$= \frac{\Delta\xi - \epsilon\zeta}{X} 2J_1\left(\frac{A}{\omega}X\right). \tag{22}$$

In obtaining the second equality of Eq. (22), we have used Eq. (18).

One can see that the effects of the driving and bias have been taken into account in our treatment, which leads to the renormalization of the significant physical properties. An interesting and key point about the CHRW method is that the CHRW Hamiltonian, Eq. (20), has the same mathematical formulation as the Rabi-RWA one except for the renormalized physical quantities. Therefore, it is mathematically straightforward to obtain the CHRW dynamics by the well-known Rabi-RWA one. We note here that the CHRW method that neglects the higher-order harmonic terms of $\tilde{H}_2$ with $n \geqslant 2$ is not a perturbation based on small tunneling, bias, or driving strength. In principle, when the driving frequency is greater than the energy splitting, i.e., $\omega \geqslant \Xi_0 = \sqrt{\Delta^2 + \epsilon^2}$, the processes involving zero and single photon are dominant. In this case, one can safely neglect the contributions from the higher-order harmonic terms in the transformed frame. When $\omega < \Xi_0 = \sqrt{\Delta^2 + \epsilon^2}$ and $A \leqslant \omega$, neglecting the high harmonic terms in the transformed Hamiltonian still yields pretty good results. We will verify these in Sec. V by detailed examination of the dynamics and the general Rabi frequency of the CHRW method with the exact numerical results. It is only when $\omega \ll \Xi_0 = \sqrt{\Delta^2 + \epsilon^2}$ and in the very strong driving case that the multiphoton processes might make considerable contributions to the dynamics and the physical quantities, and in this case the higher harmonic terms in $\tilde{H}_2$ can not be completely omitted. Thus our CHRW method is a reliable and effective approach to investigate the bias-modulated Rabi model in a wide range of parameters.

In the following, we calculate an important property in the driven dynamics, namely the occupation probability $P_{\rm up}(t)$ [33] in the CHRW method. $P_{\rm up}(t)$ denotes the probability for the system at time t to be in the spin-up state of the σ_z operator in the original spin basis of Eq. (1) while it is initially in the spin-down state of the same σ_z operator [i.e., $P_{\rm up}(0) = 0$]. Because the generator S is a function of $\sin(\omega t)$, the initial system state is the same as that in the unitarily transformed frame, namely, $|\Psi'(0)\rangle = |\Psi(0)\rangle$. Since we have also used a unitary matrix U to obtain $H_{\rm CHRW}$, the corresponding system states $|\tilde{\Psi}(t)\rangle = U^\dagger|\Psi'(t)\rangle$ satisfies the Schrödinger equation,

$$i\frac{d}{dt}|\tilde{\Psi}(t)\rangle = H_{\rm CHRW}|\tilde{\Psi}(t)\rangle. \tag{23}$$

Let us write $|\tilde{\Psi}(t)\rangle$, in terms of the eigenstates of the τ_z operator as $|\tilde{\Psi}(t)\rangle = c_1(t)|s_1\rangle + c_2(t)|s_2\rangle$ with $\tau_z|s_1\rangle = -|s_1\rangle$ and $\tau_z|s_2\rangle = |s_2\rangle$. Substituting it back to the Schrödinger equation (23), we can readily solve for $c_1(t)$ and $c_2(t)$ for the initial condition of the TLS being in the spin-down state of σ_z, i.e., $\langle\sigma_z(0)\rangle = -1$, which corresponds to $c_1(0) = -u, c_2(0) = -v$, as [48]:

$$\begin{aligned} c_1(t) = e^{i\frac{\omega t}{2}}\Bigg\{ &-u\left[\cos\left(\frac{\Omega_{\rm R}t}{2}\right) + i\frac{\tilde{\delta}}{\Omega_{\rm R}}\sin\left(\frac{\Omega_{\rm R}t}{2}\right)\right] \\ &+ iv\frac{\tilde{A}}{\Omega_{\rm R}}\sin\left(\frac{\Omega_{\rm R}t}{2}\right)\Bigg\}, \end{aligned} \tag{24}$$

$$\begin{aligned} c_2(t) = e^{-i\frac{\omega t}{2}}\Bigg\{ &-v\left[\cos\left(\frac{\Omega_{\rm R}t}{2}\right) - i\frac{\tilde{\delta}}{\Omega_{\rm R}}\sin\left(\frac{\Omega_{\rm R}t}{2}\right)\right] \\ &+ iu\frac{\tilde{A}}{\Omega_{\rm R}}\sin\left(\frac{\Omega_{\rm R}t}{2}\right)\Bigg\}, \end{aligned} \tag{25}$$

where

$$\Omega_{\rm R} = \sqrt{\tilde{\delta}^2 + \tilde{A}^2}, \tag{26}$$

$$\tilde{\delta} = \widetilde{\Xi} - \omega \tag{27}$$

are, respectively, the modulated Rabi frequency and the renormalized detuning parameter of the CHRW method. Thus, the population of the spin-up state $\binom{1}{0}$ in the σ_z basis at time t for initial $P_{\rm up}(0) = 0$ is $P_{\rm up}^{\rm CHRW}(t) = \langle\Psi(t)|\frac{\sigma_z+1}{2}|\Psi(t)\rangle$, in which

$$\begin{aligned} \langle\Psi(t)|\sigma_z|\Psi(t)\rangle = \langle\tilde{\Psi}(t)|U^\dagger e^{S(t)}\sigma_z e^{-S(t)}U|\tilde{\Psi}(t)\rangle &= \left\{1 - \frac{\zeta^2}{X^2}[1 - \cos\Theta(t)]\right\}\{(v^2 - u^2)(|c_1|^2 - |c_2|^2) - 2uv(c_2^*c_1 + c_1^*c_2)\} \\ &- \frac{\xi\zeta}{X^2}[1 - \cos\Theta(t)]\{2uv(|c_1|^2 - |c_2|^2) - (v^2 - u^2)(c_2^*c_1 + c_1^*c_2)\} - \frac{\zeta}{X}\sin\Theta(t)i(c_2^*c_1 - c_1^*c_2). \end{aligned} \tag{28}$$

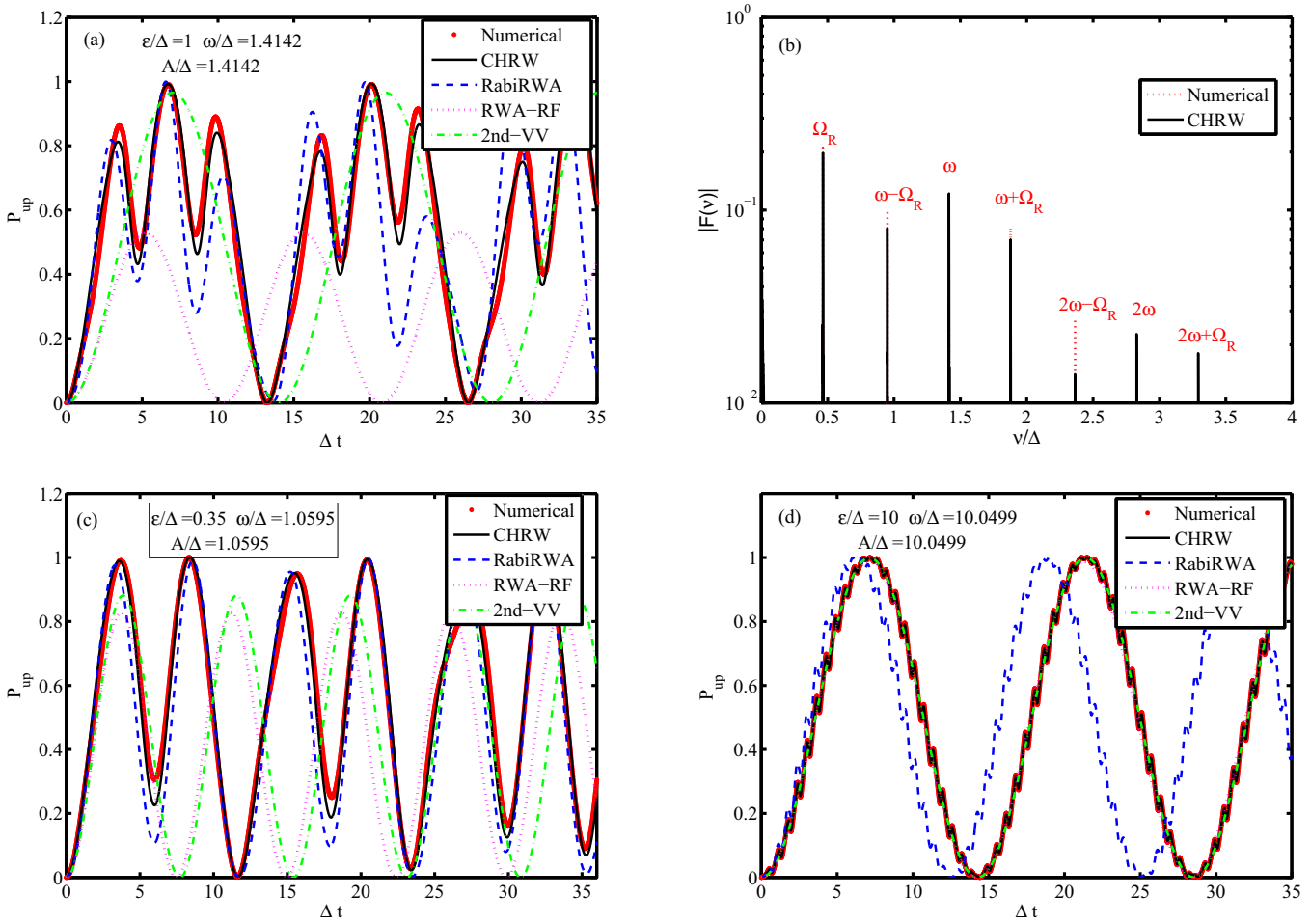

FIG. 1. Time evolutions of $P_{\rm up}(t) = \langle \frac{\sigma_z(t)+1}{2} \rangle$ as a function of Δt for different values of the bias (a) $\epsilon/\Delta = 1.0$, (c) 0.35, and (d) 10 in the on-resonance case ($\omega = \Xi_0 = \sqrt{\Delta^2+\epsilon^2}$). The driving strength A is set to be $A/\Xi_0 = 1$. The Fourier transform $F(\nu)$ of $P_{\rm up}(t)$ in (a) is shown in (b) with a discrete set of frequency components.

Note that c_1 and c_2 are time dependent and their expressions are given, respectively, in Eqs. (24) and (25), and the parameters Θ and X are defined, respectively, in Eqs. (4) and (6). The general renormalized Rabi frequency $\Omega_{\rm R}$ of Eq. (26) has taken into account the effects of CR terms and static bias on frequency shifts and will give the Bloch-Siegert shift in a simple way (will be described in Sec. IV). Physically, the renormalized quantities in the transformed Hamiltonian Eq. (20) can be detected from the general Rabi frequency and the Bloch-Siegert shift.

As discussed in our previous work [45], we demonstrated clearly that the result of the RWA-RF method [40] is a limiting case of the CHRW method for the zero bias case. For the resonance condition $n\omega + \epsilon = 0$ to hold, only one value of n is kept in the RWA-RF approach. One usually identifies the kind of resonance with a given value of n as an n-photon process. For example, the Rabi-RF resonance condition for the case $n = -1$ means $\epsilon = \omega$ (the difference from the traditional condition $\omega = \Xi_0 = \sqrt{\Delta^2+\epsilon^2}$ in the Rabi-RWA case will become clear shortly). Therefore, the effective RWA-RF Hamiltonian is written as

$$H_{\rm RWA-RF} = -J_n\left(\frac{A}{\omega}\right)\frac{\Delta}{2}\sigma_x. \tag{29}$$

Thus, the probability $P_{\rm up}(t)$ of the RWA-RF approach in Ref. [33] is obtained as

$$P_{\rm up}^{\rm RWA-RF}(t) = \sin^2\left\{J_n\left(\frac{A}{\omega}\right)\frac{\Delta t}{2}\right\} \tag{30}$$

whose amplitude is always one for any driving parameter. With parameters satisfying the resonance condition, the oscillation frequency is $J_n(\frac{A}{\omega})\Delta$. This means that the $P_{\rm up}(t)$ always exhibits a full periodic oscillation between the up and down states of σ_z except the CDT case where $P_{\rm up}^{\rm RWA-RF}(t) \equiv 0$ due to $J_n(\frac{A}{\omega}) = 0$. Therefore, the result of Eq. (30) of the RWA-RF approach is distinguished from that of the CHRW method [c.f. Eq. (28)]. This treatment simply corresponds to the case $\xi = 1$ and $\zeta = 0$ of the CHRW method, which is only valid in the limit of a really strong driving strength ($A \gg \omega, \Delta$) and with the condition $|n\omega + \epsilon| = 0$. Moreover. in Ref. [40], the Van Vleck perturbation theory is used to get the survival probability to second order in Δ for a finite static bias. We will show in the next section that the CHRW method gives a significantly better description of the system dynamics than the previous RWA or perturbative treatments as compared with the numerically exact results.

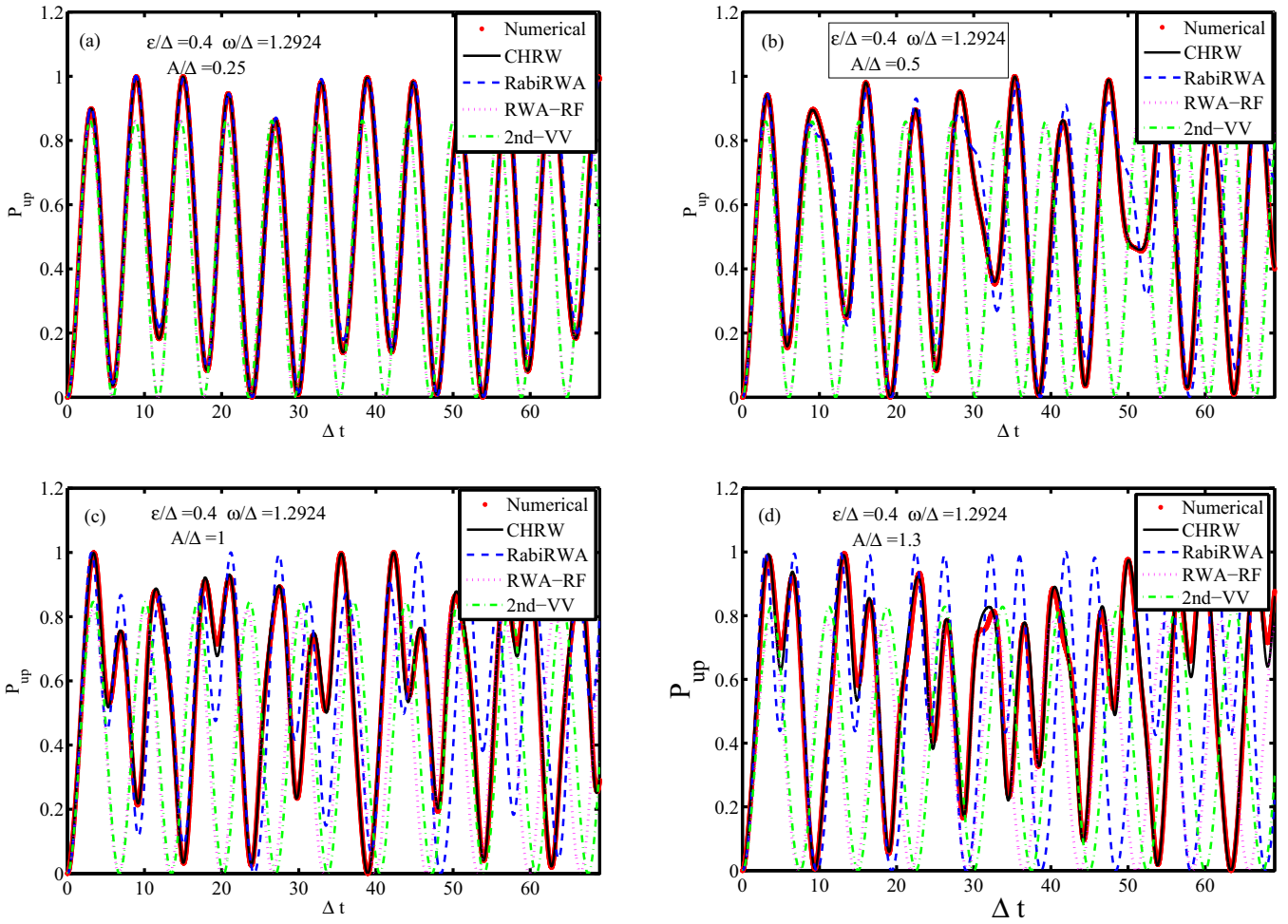

FIG. 2. Time evolutions of $P_{\rm up}(t) = \langle \frac{\sigma_z(t)+1}{2} \rangle$ as a function of Δt for different values of the driving strength (a) $A/\Delta = 0.25$, (b) 0.5, (c) 1.0, and (d) 1.3 in the near-resonance case ($\omega = 1.2\Xi_0 = 1.2924\Delta$). The bias ϵ is set to be a fixed value of $\epsilon/\Delta = 0.4$.

III. DRIVEN QUANTUM DYNAMICS

We systematically discuss here the dynamics of the driven TLS with a bias in different parameter regimes: at resonance, near resonance, and far-off resonance. With the increase of the driving strength from the weak- to strong-coupling regime, a rich distinct dynamics can be observed. We also compare all the results of the CHRW approach with those of the other methods, namely, the Rabi-RWA method, the RWA-RF method, the 2nd-VV perturbation method and the numerically exact method. Moreover, we discuss the results of time evolutions through a frequency spectrum analysis to show the accuracy of our CHRW method.

A. At resonance and near resonance

The bias modulates the energy levels of the TLS and therefore modulates the resonant condition between a driving field and the TLS. Let us take a look at the dynamics at resonance ($\omega = \Xi_0$) and near resonance ($\omega \sim \Xi_0$) for the small to large bias cases. In Fig. 1, we show the occupation probability at resonance with $A/\omega = 1$. For comparison, we also give the results of the other different approaches. One can see that the results of the CHRW are in good agreement with the numerically exact results. While the Rabi-RWA method works for $\epsilon/\Delta < 1$ with small deviation in amplitude from the numerically exact one [see Fig. 1(c)], the results of the Rabi-RF and 2nd-VV methods give different frequencies of oscillation from the numerically exact result. Nevertheless, the Rabi-RF and 2nd-VV could correctly predict the frequency of main oscillation for $\epsilon/\Delta \gg 1$ but could not give correctly the small wiggling amplitudes of the fast oscillations shown in Fig. 1(d). When $\epsilon/\Delta = 1$, the population probabilities $P_{\rm up}(t)$ obtained by the Rabi-RWA, Rabi-RF, and 2nd-VV methods all show considerable difference from the exact numerical result [see Fig. 1(a)]. But the CHRW result still agrees rather well with the corresponding numerical result. In Fig. 1(b), we show the Fourier transform of the $P_{\rm up}(t)$ in Fig. 1(a):

$$F(\nu) = \int_{-\infty}^{\infty} dt\, P_{\rm up}(t) \exp(i\nu t). \tag{31}$$

The values (or positions) of the discrete frequencies obtained by the CHRW method are precisely the same as those obtained by the numerically exact method. One can see that there exist two dominating oscillation frequencies with larger weight, one corresponding to the driving frequency $\omega/\Delta = \sqrt{2}$ and the other corresponding to the Rabi frequency $\Omega_{\rm R}/\Delta = 0.4643$. Moreover, there are the components of the frequencies $n\omega \pm$

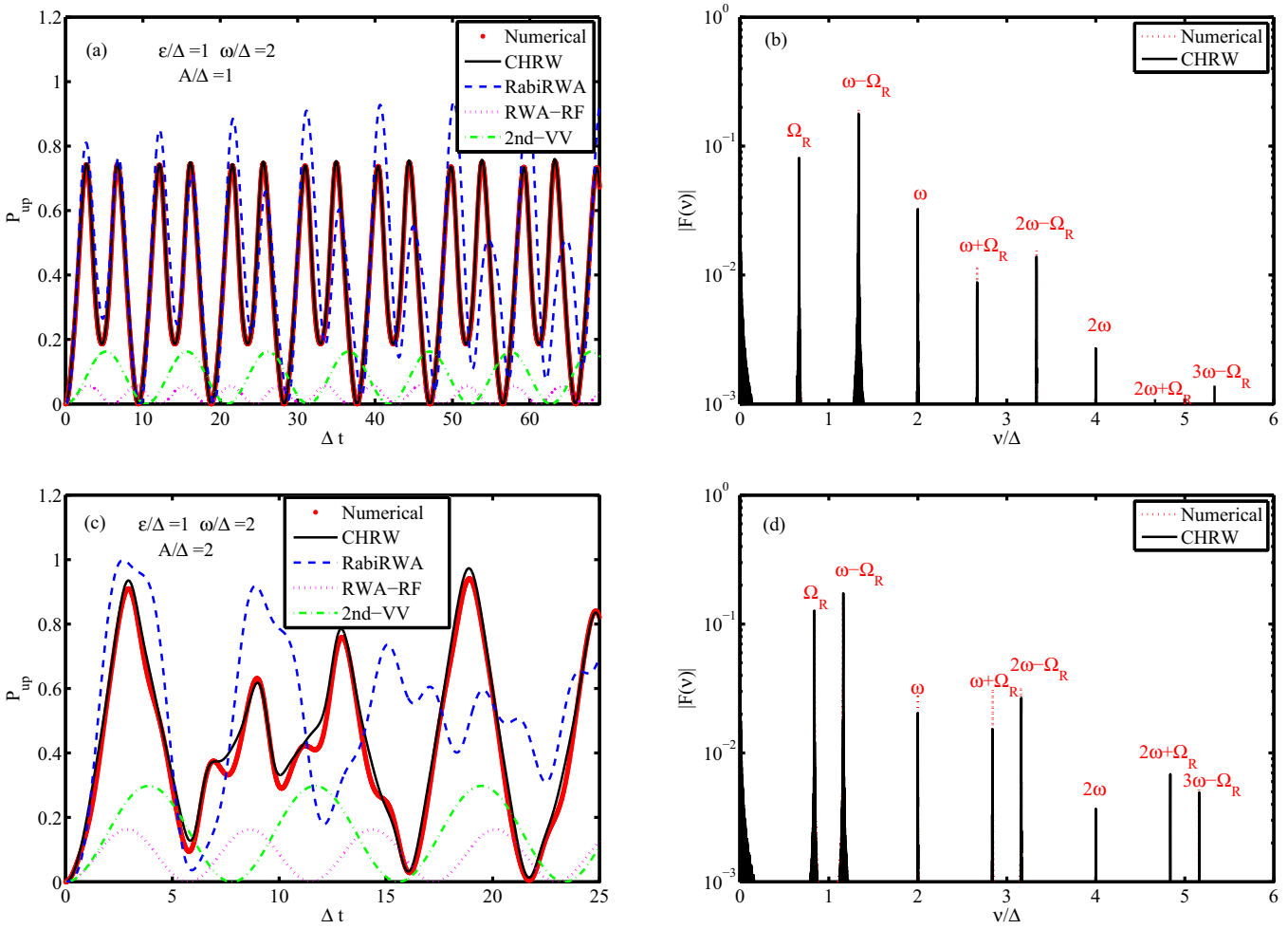

FIG. 3. Time evolutions of $P_{\rm up}(t) = \langle \frac{\sigma_z(t)+1}{2} \rangle$ as a function of Δt for different values of the driving strength (a) $A/\Delta = 1$, and (c) $A/\Delta = 2$ in the off-resonance case ($\omega = 2\Delta > \Xi_0$). The corresponding Fourier transform $F(\nu)$ of $P_{\rm up}(t)$ in (a) and (c) is shown in (b) and (d), respectively. The bias ϵ is set to be $\epsilon/\Delta = 1$.

$\Omega_{\rm R}$ ($n \geqslant 1$) and $m\omega$ ($m \geqslant 2$) with small weight, which are consistent with the formula in Eq. (28).

We show the near-resonance dynamics ($\omega = 1.2\Xi_0 = 1.2924\Delta$) for several moderate driving strengths in Fig. 2. It is easy to check that for a very weak driving strength the results of all methods are nearly the same [see Fig. 2(a)]. However, the Rabi-RWA method breaks down when $A/\Delta > 0.5$ [see Figs. 2(c)–2(d)]. Meanwhile, the deviation of the RWA-RF and 2nd-VV results from the numerically exact results becomes much larger with the increase of the driving strength [see Figs. 2(b)–2(d)]. In contrast, our CHRW method works quite well for all the parameters used in Fig. 2. The time evolutions of $P_{\rm up}^{\rm CHRW}(t)$ are in quantitatively good agreement with numerically exact results when the driving strength increases from a small value to $A \sim \Xi_0$ or even to $A = 1.5\Delta$.

From all the above figures, one can see that the CHRW captures correctly the characters of the on-resonance and near-resonance dynamics. By comparison with the numerical results, the CHRW treatment gives a significantly better description than the other treatments. Physically, the CHRW method takes into account the effects of the bias and the driving on equal footing. The combined effects result in the renormalization of the physical quantities in the transformed CHRW Hamiltonian [see Eq. (20)]. For example, in the near-resonance case of $\omega/\Xi_0 = 1.2(\epsilon/\Delta = 0.4)$ with $A/\Delta = 1.3$ of Fig. 2(d), we obtain $\zeta = 0.1855$ and $\xi = 0.6279$ by self-consistently solving Eq. (18) and Eq. (19). Thus we get the renormalized physical quantities $\widetilde{A} = 0.5273\Delta$ and $\widetilde{\Xi} = 1.0085\Delta$. One can see from Fig. 2(d) that the time evolution of the CHRW method is quantitatively in good agreement with the numerically exact result, but the Rabi-RWA, averaged second-order VV, and RWA-RF results show large deviation from the numerically exact result. Due to the renormalization, the TLS $P_{\rm up}(t)$ of Eq. (28) yields the correct driven tunneling dynamics. Thus, the CHRW method is a simple tractable method that allows us to study the influence of the bias and CR terms on the dynamics and the physics in the parameter regime where the Rabi-RWA and RWA-RF methods fail, especially the moderately strong driving-strength regime with $A \sim \omega \sim \epsilon \sim \Delta$.

B. Off resonance

Next, we show the time evolutions of $P_{\rm up}(t)$ in the off-resonance case of $\omega = 2\Delta > \Xi_0$ with $\epsilon/\Delta = 1$ for two moderately strong driving strengths $A/\Delta = 1$ and $A/\Delta = 2$ in Figs. 3(a) and 3(c), respectively. At the same time, we also

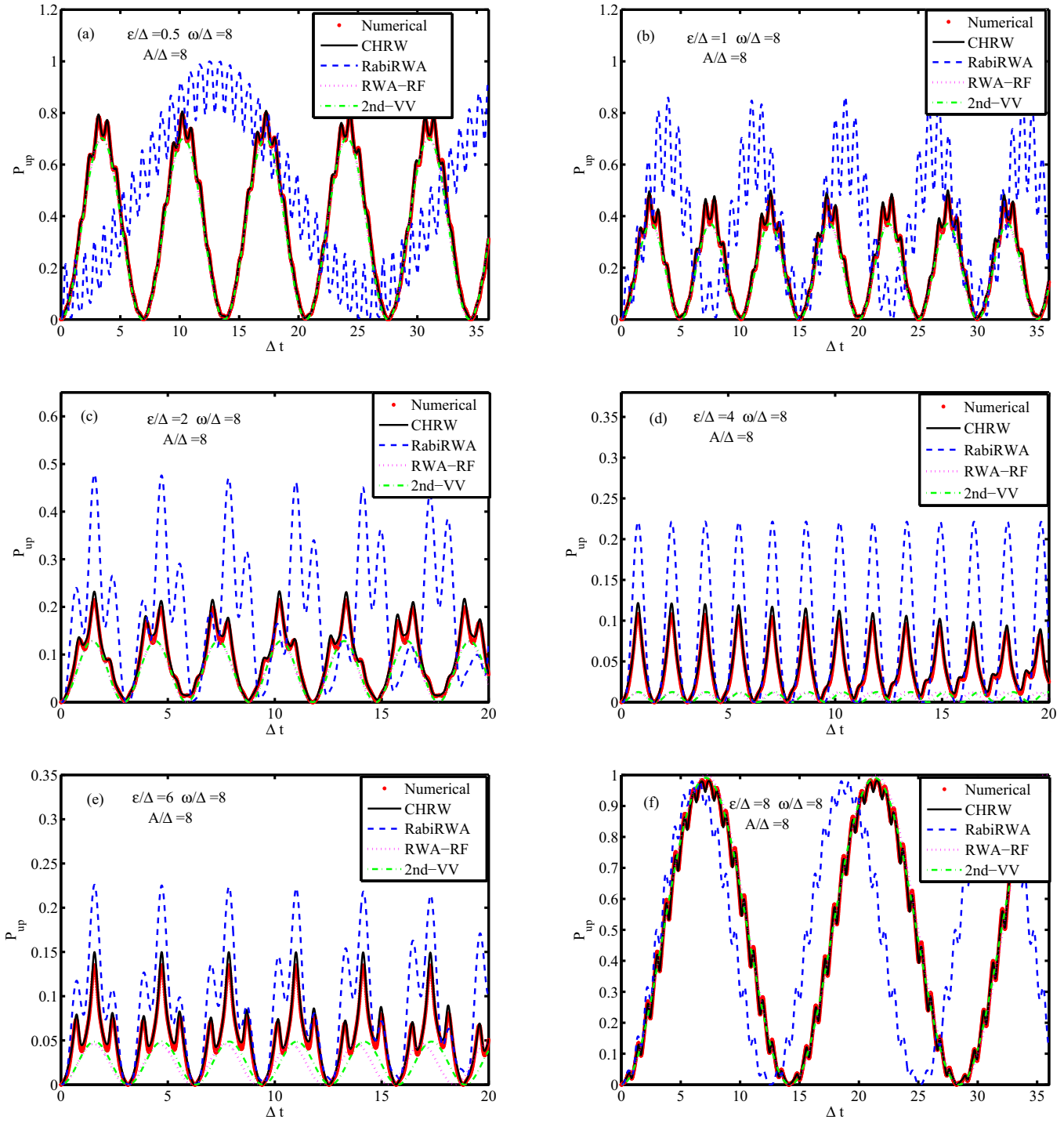

FIG. 4. Time evolutions of $P_{\rm up}(t) = \langle \frac{\sigma_z(t)+1}{2} \rangle$ as a function of Δt for different values of the bias (a) $\epsilon/\Delta = 0.5$, (b) 1, (c) 2, (d) 4, (e) 6, and (f) 8 in the off-resonance case ($\omega = 8\Delta \neq \Xi_0$). The driving strength A is set to be $A/\omega = 1$ ($A/\Delta = 8$).

show the corresponding Fourier transform with a discrete set of frequency components in Figs. 3(b) and 3(d). For $A/\Delta = 1$, the dynamics of the the CHRW method agrees quite well with the numerically exact ones, which can be confirmed by the consistence of their frequency components as shown in Fig. 3(b). The dynamics of the Rabi-RWA exhibits some deviation in oscillation amplitude from but with the main oscillation frequency close to the exact numerical results in Fig. 3(a). On the other hand, the main oscillation frequencies of the RWA-RF and second-order VV results are substantially different from that of the exact result. As the driving strength increases up to $A/\Delta = 2$, the CHRW method still gives a correct dynamics with only small errors in amplitude [see Figs. 3(c) and 3(d)]. In contrast, the other analytical methods could not give the accurate oscillations and Rabi frequency.

In Fig. 4, we show the effects of the bias on the dynamics of the driven system for the off-resonance ($\omega = 8\Delta \neq \Xi_0$) and strong driving ($A = \omega = 8\Delta$) cases. In comparison with

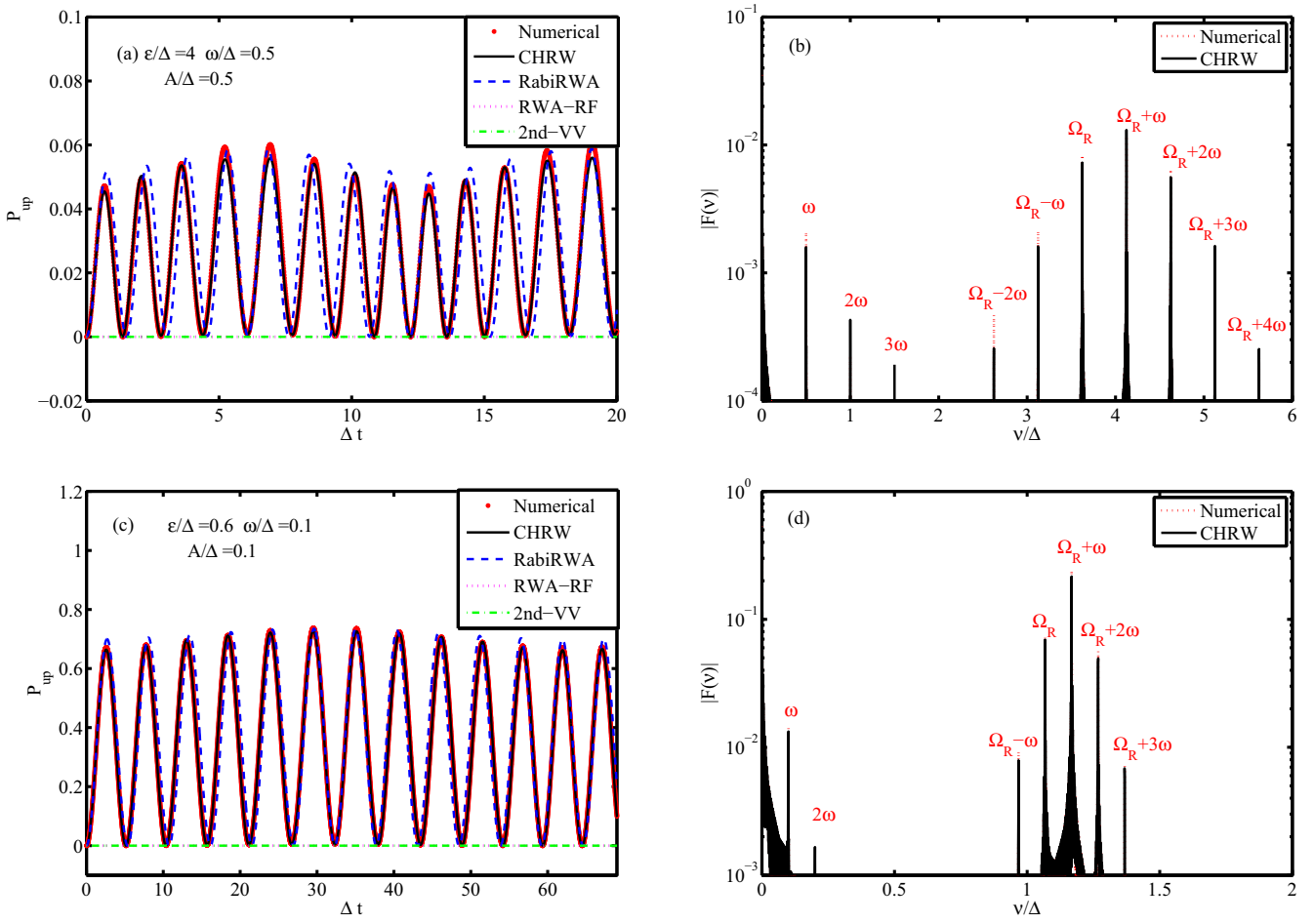

FIG. 5. Time evolutions of $P_{\rm up}(t) = \langle \frac{\sigma_z(t)+1}{2} \rangle$ as a function of Δt for different values of the bias (a) $\epsilon/\Delta = 4$, and (c) 0.6 in the off-resonance case ($\omega < \Xi_0$). The corresponding Fourier transform $F(\nu)$ of $P_{\rm up}(t)$ in (a) and (c) is shown in (b) and (d), respectively. The driving strength is set to be $A/\omega = 1$.

the exact results, the CHRW method gives not only the main oscillations but also the time evolution of tiny higher harmonic frequency right for all the cases of Figs. 4(a)–4(f). In contrast, the Rabi-RWA approach fails apparently in the strong driving cases. The RWA-RF and the 2nd-VV results have the main oscillations close to those of the exact numerical results for almost all the cases, while they can not show the fine structures in the time evolutions. Furthermore, the oscillation amplitudes of the RWA-RF and the 2nd-VV results in Figs. 4(d) and 4(e) are considerably smaller than those of the exact numerical results.

We show the time evolutions of $P_{\rm up}(t)$ as well as the corresponding Fourier transform for the off-resonance case of $\omega < \Xi_0$ in Fig. 5. In the large bias case of $\epsilon = 4\Delta$ in Fig. 5(a) with $A = \omega = 0.5\Delta$, we solve the Rabi frequency, Eq. (26), and obtain $\Omega_{\rm R}/\Delta = 3.6238 \gg \omega/\Delta = 0.5$. The frequency of amplitude envelope of the driven dynamics in Fig. 5(a) is 0.5Δ. On the other hand, in the small bias case of $\epsilon = 0.6\Delta$ in Fig. 5(c) with $A = \omega = 0.1\Delta$, we get the Rabi frequency $\Omega_{\rm R}/\Delta = 1.0677 \gg \omega/\Delta = 0.1$. By the Fourier transform of the time evolutions, we show in Figs. 5(b) and 5(d) the discrete frequencies are $n\omega$ and $\Omega_{\rm R} \pm n\omega$ ($n = 0,1,2,\ldots$). The dominant oscillation frequency is neither ω nor $\Omega_{\rm R}$. It is $\Omega_{\rm R} + \omega$ with the largest weight for the parameters in Fig. 5. Besides, the Rabi-RWA results agree roughly with the exact results, but the RWA-RF and 2nd-VV results show $P_{\rm up}(t) = 0$ without any oscillation in contrast with the numerical results. In other words, in this parameter regime of $A\omega/\Delta^2 < 1$, the RWA-RF and the 2nd-VV methods are invalid.

IV. GENERALIZED RABI FREQUENCY

We discuss and calculate the generalized Rabi frequency and the Bloch-Siegert shift and compare our calculated values with the data shown in the experiment of flux qubit [44]. First, we derive, for simplicity, a formula of the Rabi frequency to second order in A based on the general Rabi frequency, Eq. (26). Then we calculate and discuss the bias-modulated Bloch-Siegert shift. Finally, we illustrate the valid parameter regime of our CHRW method.

A. Frequency shift: Bloch-Siegert shift

In the following, we shall address the question of whether the bias leads to a profound change of the Rabi frequency and the shift of the resonance frequency. To this end, in this subsection we calculate the generalized Rabi frequency and bias-modulated Bloch-Siegert shift analytically and numerically. From Eqs. (26), (27), (22), (16), (11), and (12), the

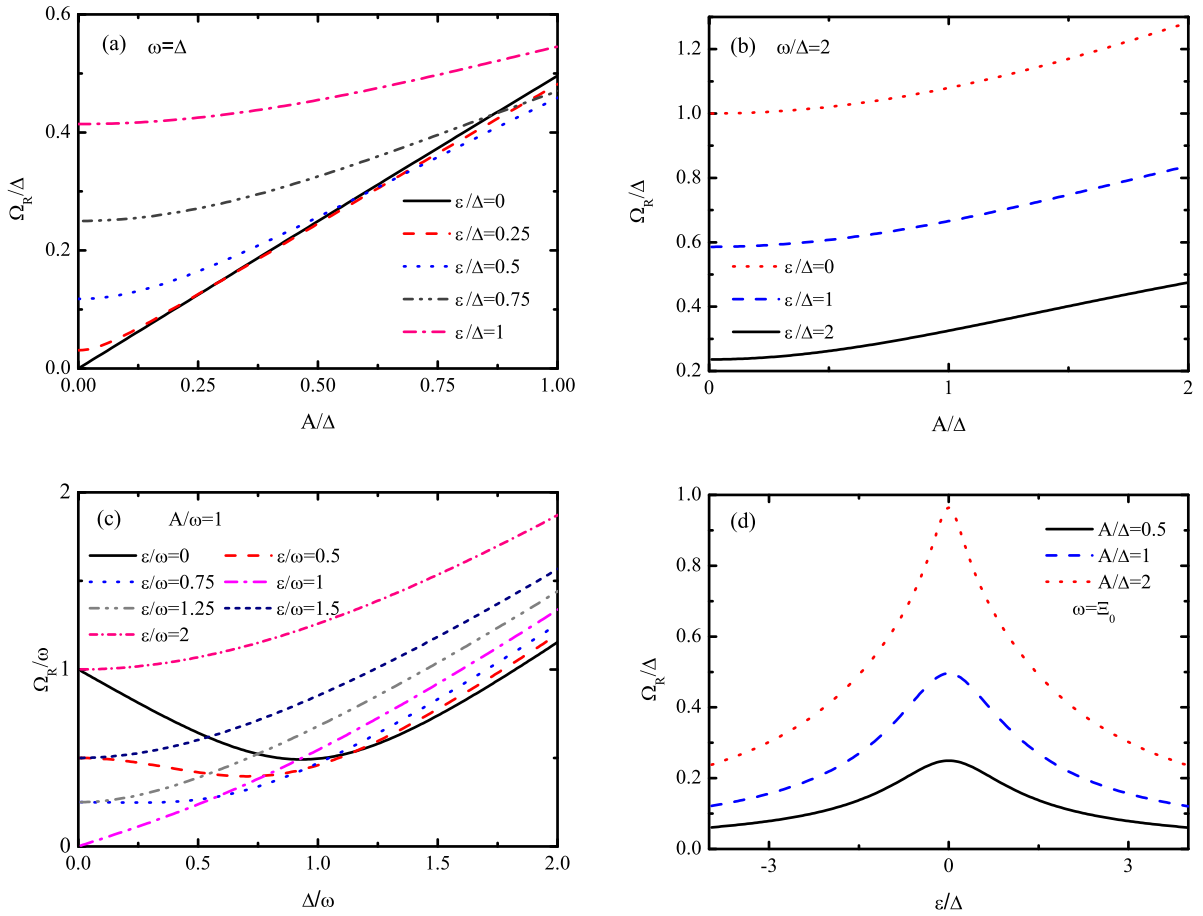

FIG. 6. (a) Generalized Rabi frequency Ω_R as a function of the driving strength A with $\omega = \Delta$ for several different values of bias $\epsilon/\Delta = 0$, 0.25, 0.5, 0.75, and 1. (b) Generalized Rabi frequency Ω_R as a function of A with $\omega = 2\Delta$ for different values of bias $\epsilon/\Delta = 0$, 1, and 2. (c) Generalized Rabi frequency Ω_R as a function of Δ with $A/\omega = 1$ for several different values of bias $\epsilon/\omega = 0$, 0.5, 0.75, 1, 1.25, 1.5, and 2. (d) Generalized Rabi frequency Ω_R as a function of the bias ϵ with $\omega = \Xi_0$ for several different values of driving strength $A/\Delta = 0.5$, 1, and 2.

general renormalized Rabi frequency that takes into account the effects of CR couplings and the bias can be written as

$$\Omega_R^2 = [\omega - \widetilde{\Xi}]^2 + \left[2\frac{\Delta\xi - \epsilon\zeta}{X} J_1\left(\frac{A}{\omega}X\right)\right]^2 = \left\{\omega - \sqrt{\Xi_0^2 - \left[1 - J_0^2\left(\frac{A}{\omega}X\right)\right]\left(\frac{\Delta\xi - \epsilon\zeta}{X}\right)^2}\right\}^2 + \left[2\frac{\Delta\xi - \epsilon\zeta}{X} J_1\left(\frac{A}{\omega}X\right)\right]^2. \quad (32)$$

For a finite bias, we will derive an analytical expression up to second order in the driving strength A. The Bloch-Siegert shift is a well-known correction to the RWA, and accounts for the CR field to leading order. Expanding ξ and ζ up to lowest order in A, we obtain from Eqs. (18) and (19)

$$\Delta\xi - \epsilon\zeta = \frac{\omega\Delta}{\omega + \Xi_0}. \quad (33)$$

Thus the modulated effective Rabi frequency to second order in A has the form

$$\Omega_{R-2nd}^2 = [\omega - \Xi_0]^2 + \frac{A^2\Delta^2}{2\Xi_0(\omega + \Xi_0)}, \quad (34)$$

whose expression in the limit of vanishing bias is the same as those given in Refs. [32] and [34]. Moreover, Eq. (34) can be used to analytically calculate the Bloch-Siegert shift of the resonance frequency Ω_{res}, which is defined as the frequency at which the transition probability average is a maximum [34]. This occurs when $\partial\Omega_R^2/\partial\Delta = 0$ [34]. Thus, we obtain the Bloch-Siegert shift $\delta\omega_{BS}$ as

$$\delta\omega_{BS} = \Omega_{res} - \Xi_0 = \frac{A^2}{4\Xi_0}\left[1 - \frac{3}{4}\left(\frac{\Delta}{\Xi_0}\right)^2\right]. \quad (35)$$

For $\epsilon = 0$, Eq. (35) reproduces the result of $\frac{1}{16}\frac{A^2}{\Delta}$ given in Ref. [34]. In the unbiased case, the Rabi frequency Ω_R up to fourth order in A has been given in our previous work [45]. Moreover, we confirm that the Bloch-Siegert shift for the unbiased case given by our method is in a good agreement with that obtained by the Floquet approach in the entire driving-strength regime [46]. These results strongly prove that the CHRW method has properly taken into account the effects of CR terms and the bias.

B. Effects of the bias on the Rabi frequency

We discuss here the dependence of the generalize Rabi frequency Ω_R on the parameters of A, Δ, and ϵ. Figure 6(a)

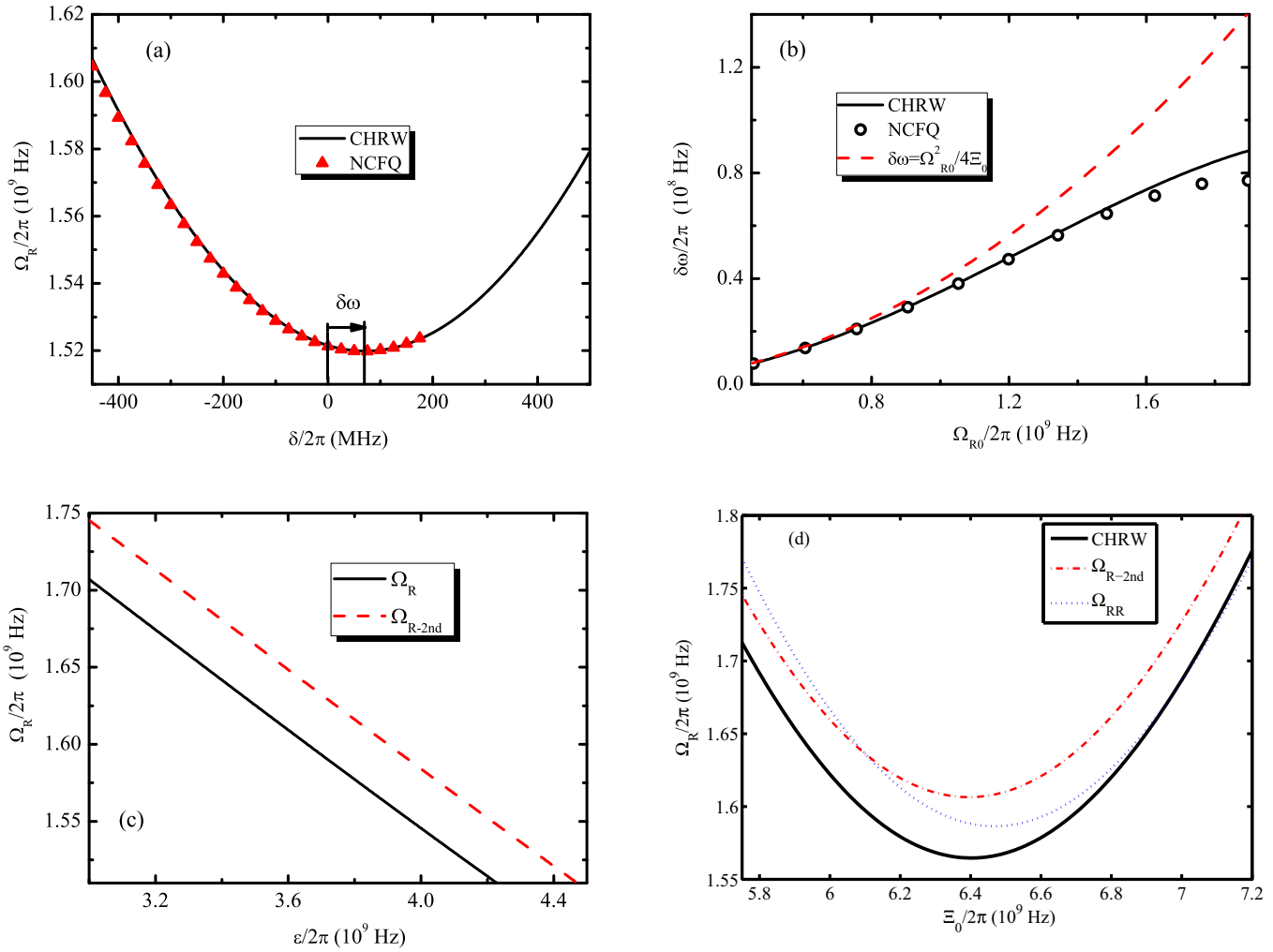

FIG. 7. (a) Generalized Rabi frequency Ω_R as a function of the detuning $\delta = \Xi_0 - \omega$ obtained by the CHRW method (black solid line) with $A/2\pi = 4.100$ GHz, $\epsilon/2\pi = 4.154$ GHz and $\Delta/2\pi = 4.869$ GHz ($\Xi_0 = 6.4$ GHz). The data for numerically calculation of the flux qubit (NCFQ) in Ref. [44] are represented by red triangles. (b) Numerically calculated frequency shift $\delta\omega$ by the CHRW method (black solid line), the second-order Bloch-Sigert shift (red dashed line) and the NCFQ results in Ref. [44] (open circles). (c) Generalized Rabi frequency Ω_R as a function of ϵ given by Eq. (34) (red dashed line) and Eq. (32) (black solid line). (d) Generalized Rabi frequency Ω_R as a function of Ξ_0 with $\omega/2\pi = 6.1$ GHz calculated by Eq. (34) (red dash-dotted line) and Eq. (32) (black solid line). The blue dotted line denotes the Rabi frequency Ω_{RR} obtained by the Rabi-RWA method.

shows Ω_R as a function of the driving strength A for various bias values and a fixed driving frequency $\omega = \Delta$. One can see that for $\epsilon = 0$, Ω_R is linearly proportional to A in the small driving-strength regime where $A/\Delta \leqslant 1$. When $A/\Delta < 0.5$, the values of Ω_R with a finite bias $\epsilon > 0$ are larger than those with $\epsilon = 0$, and increases with the increase of the bias. When $A/\Delta > 0.5$, however, the crossover of the curves for different values of the bias ϵ appears. In this regime, the increase of the bias does not always favor the increase of Ω_R. This comes from the competition between different controlled parameters (ϵ/Δ,ω/Δ, and A/Δ). It indicates that the relation of Ω_R versus A is beyond a linear dependent behavior when all the energy scales are nearly in the same order. Figure 6(b) displays the Rabi frequency Ω_R as a function of the driving strength A for three values of bias ϵ and a fixed driving frequency $\omega = 2\Delta$. Obviously, the increase of the bias ϵ decreases the Rabi frequency Ω_R in this parameter regime.

In Fig. 6(c), we show the dependence of the Rabi frequency Ω_R on Δ for different values of the bias ϵ with $A/\omega = 1$. For $\epsilon = 0$, the position of the scaled tunneling Δ/ω corresponding to the minimum value of Ω_R is not located at $\Delta/\omega = 1$ but at $\Delta/\omega = 0.93$. This indicates that the CR terms lead to the explicit deviation from the RWA result of $\Delta/\omega = 1$ in the intermediate driving-strength regime. For finite bias case ($0 < \epsilon \leqslant 0.5\omega$), with the increase of Δ/ω, Ω_R falls first and then rises. For $\epsilon/\omega = 0.75$, Ω_R is insensitive to the change of the scaled tunneling when $\Delta/\omega \leqslant 0.5$ in comparison with its fast increase when $\Delta/\omega \geqslant 1$. For $\epsilon/\omega \geqslant 1$, Ω_R generally increases with the increase of the scaled tunneling. We notice that near $\Delta/\omega \sim 1$, Ω_R is almost the same for $\epsilon/\omega < 1$. Moreover, when $\Delta/\omega > 1.25$, Ω_R increases with the increase of the bias in contrast to its nonmonotonic dependence on bias when $\Delta/\omega < 0.5$. This indicates that the competition between the quantum tunneling Δ/ω and the driving A/ω leads to the complicated

dependence of Ω_R on the bias ϵ in the intermediate driving-strength regime.

In Fig. 6(d), we show the Rabi frequency Ω_R as a function of the bias ϵ at $\omega = \Xi_0$ for different driving strengths. Ω_R displays a parity symmetry with respect to the bias ϵ, i.e., $\Omega_R(-\epsilon) = \Omega_R(\epsilon)$, which can be seen, for example, by Eq. (37) valid to second order in A. When the bias ϵ is fixed, the larger the driving strength A, the larger the Rabi frequency Ω_R. When A is set to a fixed value, Ω_R decreases with increasing the absolute value of ϵ, and Ω_R reduces more drastically for $A/\Delta = 2$ than $A/\Delta = 0.5$.

Present calculated results may be examined and compared to available experimental measurements of superconducting flux qubits. In order to show the effects of the bias on the generalized Rabi frequency in the flux qubit, we use the parameters of the flux qubit in Ref. [44], $\Delta/2\pi = 4.869\,\mathrm{GHz}$ and $\epsilon/2\pi = 4.154\,\mathrm{GHz}$ ($\Xi_0/2\pi = 6.400\,\mathrm{GHz}$). In Fig. 7(a), we plot Rabi frequency Ω_R as a function of $\delta = \omega - \Xi_0$. The minimum of the Rabi frequency is not located at $\delta = 0$, but at $\delta\omega/2\pi = 70\,\mathrm{MHz}$, which is very close to the value $\delta\omega/2\pi = 66.5\,\mathrm{MHz}$ given in Ref. [44]. One can see that our results are in good agreement with the numerically calculated data of the flux qubit (NCFQ) in the whole parameter regime presented in Ref. [44]. Figure 7(b) displays the frequency shift as a function of $\Omega_{R0} \equiv \frac{\Delta}{2}\frac{A}{\Xi_0}$ together with the second-order Bloch-Siegert shift [6,34], $\delta\omega_{BS}^{2nd} = \frac{1}{4}\frac{\Omega_{R0}^2}{\Xi_0}$. It is obvious that $\delta\omega_{BS}^{2nd}$ overestimates $\delta\omega$ when $\Omega_{R0}/2\pi \geqslant 0.8\,\mathrm{GHz}$. Our CHRW results are in close agreement with the results in Ref. [44]. The deviation from the Bloch-Siegert shift comes from the combined effects of the driving and the static bias.

We compare in Fig. 7(c) the generalized Rabi frequency Ω_R, Eq. (32), as a function of bias ϵ with the second-order result of Eq. (34). The curves given by Eq. (32) and Eq. (34) have the same slope in the parameter regime of Fig. 7(c). The generalized Rabi frequency Ω_R versus ϵ manifests a linear relation between them in the resonance case, which can be shown by both Eq. (32) and Eq. (34). We find that the second-order perturbation results given by Eq. (34) agree well with the calculated result of Fig. 1(c) in Ref. [44] obtained by a fit formula based on the linear approximation.

Figure 7(d) shows the Rabi frequencies as a function of Ξ_0 with a fixed tunneling strength $\Delta/2\pi = 4.869\,\mathrm{GHz}$ obtained by three methods: the CHRW method (the black solid line), the second-order approximation of the CHRW method (the red dash-dotted line), and the Rabi-RWA method (the blue dotted line). For a fixed driving frequency $\omega/2\pi = 6.1\,\mathrm{GHz}$, both Ω_R and Ω_{R-2nd} have a minimum approximately located at $\Xi_0/2\pi = 6.4\,\mathrm{GHz}$, near which the Rabi frequencies are insensitive to the bias $\epsilon = \sqrt{\Xi_0^2 - \Delta^2}$. In contrast, the minimum of Ω_{RR} occurs at a position very close to $\Xi_0/2\pi = 6.5\mathrm{GHz}$, larger than those of Ω_R and Ω_{R-2nd}. This difference is attributed to the combined effects of the bias and the driving.

C. Valid parameter regime of the CHRW method

In this subsection, we discuss the parameter regime in which the CHRW method is valid in comparison with those of the other approaches. The Rabi-RWA approach, which neglects the CR interactions works well in the weak-driving limit. The CHRW method covers the the parameter regimes that are good for the Rabi-RWA method, which is perturbative in the driving strength [37]. In the unbiased or small bias case ($\epsilon \ll \Delta$), the CHRW method works very well for $A/\omega \leqslant 2$ as shown in Fig. 6 of Ref. [45]. When $\epsilon \simeq \Delta$, it gives accurate results in the parameter space $A/\omega \leqslant 1$ regardless of the value of ω. In comparison with the exact numerical results, the CHRW method works also very well for the larger bias case $\epsilon \gg \Delta$ (such as $\epsilon/\Delta \geqslant 10$) with a fixed driving frequency $\omega = \Delta$ and the driving strength in the regime of $A/\omega \leqslant 2$. More interestingly, the CHRW method can give the correct results when the values of the driving parameters(ω and A) are comparable to those of the energy scales (Δ and ϵ). For example, the regime $A\omega/\Delta^2 \leqslant 1$ in which the second-order VV method and RWA-RF (see Fig. 5) fail is in the valid parameter regime of the CHRW method. Moreover, the CHRW method works very well also in the parameter regime $A\omega/\Delta^2 \gg 1$ in which the RWA-RF method is valid (see Fig. 4).

V. SUMMARY

We have developed a CHRW method to systematically investigate the driven dynamics of a TLS under a periodic driving field and a static bias. This CHRW method treats the driving field and the bias on equal footing by a unitary transformation. The transformed Hamiltonian in the eigenbasis of the zero-photon Hamiltonian H_0' takes a simple RWA form after we properly choose the parameters ξ and ζ in the unitary transformation by the self-consistent equations (18) and (19) and neglect the H_2' that involves all multi-ω terms or multiphoton assisted transitions ($n\omega$, $n = 2,3,4,\ldots$). Physically, all the results are dependent on the renormalized energy splitting $\tilde{\Xi}$ and the renormalized (modified) driving strength $\tilde{A}$ in the transformed RWA Hamiltonian. The renormalization of these two parameters $\tilde{\Xi}$ and $\tilde{A}$ comes from the combined effect among the tunneling of the TLS, the driving field and the bias. The CHRW method allows us to analytically calculate the driven tunneling dynamics in the renormalized rotating-wave framework, so as the generalized bias-modulated Rabi frequency and the frequency shift including the Bloch-Siegert shift.

We have demonstrated the effects of the driving field and the bias on the system dynamics and the generalized Rabi frequency. We have not only given the small-bias and weak-driving strength results, such as the Rabi physics, but also shown the strong driving strength and large bias results, such as the nonsinusoidally complicated time evolutions. From the driven tunneling dynamics, one can see that the characteristics of the oscillations are very sensitive to $\widetilde{A}$ and $\widetilde{\Xi}$. Compared to other analytical methods, the CHRW method can give the correct and accurate dynamics in good agreement with the numerically exact results in a broad region of the parameter space and still preserves the merits of the simple RWA mathematical form in the final transformed Hamiltonian. Unlike the conventional Rabi-RWA method, the CHRW technique is nonperturbative in driving strength, so it can be applied to study the driven tunneling physics in a broader parameter regime, especially beyond the weak driving regime and the small bias and near resonance cases. In a wide range values of the Δ, ϵ, A and ω parameters, we have compared the dynamics obtained by the CHRW

method with that by the numerically exact method. We have found and confirmed that the CHRW method works very well even for the (moderately) strong driving strength region. The contribution to the dynamics of the multi-ω terms or multiphoton assisted transitions ($n\omega$, $n = 2,3,4,\ldots$) we have neglected is not prominent except for the ultrastrong driving strength case. Thus it gives the accurate driven dynamics in the parameter regimes of ($\epsilon/\Delta \ll 1$ or $\gg 1$, $\Delta/\omega < 1$, $A/\omega \leqslant 2$) and ($\epsilon/\Delta \sim 1$, $\Delta/\omega \sim 1$, $A/\omega \leqslant 1$), and in the neighboring regimes the driven tunneling dynamics though not exact is in qualitative agreement with that of the numerical method. By Fourier transform analysis, the discreet frequency values in $P_{\rm up}(t)$ of the CHRW results match very well the ones obtained by the exact numerical method. More interestingly, the CHRW approach can directly give an analytical expression for the generalized Rabi frequency $\Omega_{\rm R}$ and can show explicitly the dependence of $\Omega_{\rm R}$ on the driving parameters, bias, and tunneling. The results obtained via the CHRW method might account for the versatile strongly driven experiments investigated in Refs. [30,35].

The CHRW method provides a simple and direct way for accurately studying the properties of driven tunneling systems with a static bias in a wide range of parameters. The approach is not an upgrade patch for the conventional RWA but a much improved innovative RWA. The theoretical results may serve as a tool kit for probing limitations and possibilities in driven physics and quantum control with obvious applications in quantum information. The CHRW method can also be applied to some complicated problems and dissipative dynamics exposed to strong ac driving [32]. For example, it will prove useful in treating the problems of multichromatically driven tunneling quantum dynamics. The work is a subject for future research.

ACKNOWLEDGMENTS

Z.L. thanks F. Yoshihara for helpful discussions. The work was supported by the National Natural Science Foundation of China (Grants No. 11474200, No. 11581240311, and No. 11374208). Z.L. gratefully acknowledges support from the National Natural Science Foundation of China to do research in ICTP (SMR2705). H.S.G. acknowledge support from the the Ministry of Science and Technology of Taiwan under Grant No. 103-2112-M-002-003-MY3, from the National Taiwan University under Grant No. NTU-ERP-104R891402, and from the thematic group program of the National Center for Theoretical Sciences, Taiwan.

APPENDIX: OCCUPATION PROBABILITY OF THE RABI-RWA

We discuss briefly how the Rabi-RWA Hamiltonian is obtained from the Hamiltonian of Eq. (1) and present the occupation probability of the driven TLS obtained by the Rabi-RWA method. Writing the transition frequency of the TLS or the flux qubit as $\Xi_0 = \sqrt{\Delta^2 + \epsilon^2}$, thus we transform the Hamiltonian in the current basis to that in the energy basis by a unitary matrix $U_0 = u_0\sigma_z - v_0\sigma_x$, in which $u_0 = \sqrt{\frac{1}{2} - \frac{\epsilon}{2\Xi_0}}$, $v_0 = \sqrt{\frac{1}{2} + \frac{\epsilon}{2\Xi_0}}$. The Hamiltonian in the energy eigenbasis is then written as $H_{\rm eig} = \frac{\Xi_0}{2}\tilde{\sigma}_z + \frac{A_x}{2}\cos(\omega t)\tilde{\sigma}_x + \frac{A_z}{2}\cos(\omega t)\tilde{\sigma}_z$, where $\tilde{\sigma}_i$ are the Pauli spin component operators in the energy basis, $A_x = (\Delta/\Xi_0)A$ and $A_z = (\epsilon/\Xi_0)A$. After dropping all the fast oscillatory terms including the last term of $\frac{A_z}{2}\cos(\omega t)\tilde{\sigma}_z$ in the Hamiltonian $H_{\rm eig}$, one obtains the Rabi-RWA Hamiltonian

$$H_{\rm Rabi-RWA} = \frac{\Xi_0}{2}\tilde{\sigma}_z + \frac{A_x}{4}[\tilde{\sigma}_+ \exp(-i\omega t) + \tilde{\sigma}_- \exp(i\omega t)], \tag{A1}$$

where $\tilde{\sigma}_\pm = (\tilde{\sigma}_x \pm i\tilde{\sigma}_y)/2$. The occupation probability $P_{\rm up}(t)$ as an important property is the probability in the spin-up eigenstate of the original σ_z operator in the Hamiltonian Eq. (1) at time t when the system is initialized in the spin-down eigenstate of the same σ_z operator [i.e., $P_{\rm up}(0) = 0$]. Since the CR terms have been neglected in Eq. (A1), we can immediately obtain after some algebra the Rabi-RWA result, $P_{\rm up}^{\rm Rabi}(t) = \frac{1+\langle\sigma_z(t)\rangle}{2}$, in which

$$\begin{aligned}\langle\sigma_z(t)\rangle^{\rm Rabi} = &-\frac{\epsilon}{\Xi_0}\left\{\frac{\epsilon}{\Xi_0}\left[1 - \frac{A_x^2}{2\Omega_{\rm RR}^2}\sin^2\left(\frac{\Omega_{\rm RR}t}{2}\right)\right] + \frac{\Delta}{\Xi_0}\frac{\delta A_x}{\Omega_{\rm RR}^2}\sin^2\left(\frac{\Omega_{\rm RR}t}{2}\right)\right\}\\ &-\frac{\Delta}{\Xi_0}\left\{\cos(\omega t)\left[\frac{\Delta}{\Xi_0} - \left(\frac{\Delta}{\Xi_0}\frac{2\delta^2}{\Omega_{\rm RR}^2} - \frac{\epsilon}{\Xi_0}\frac{\delta A_x}{\Omega_{\rm RR}^2}\right)\sin^2\left(\frac{\Omega_{\rm RR}t}{2}\right)\right] - \sin(\omega t)\frac{\Delta\delta - \epsilon A_x/2}{\Xi_0\Omega_{\rm RR}}\sin(\Omega_{\rm RR}t)\right\},\end{aligned} \tag{A2}$$

where $\delta = \Xi_0 - \omega$ is the detuning parameter and $\Omega_{\rm RR} = \sqrt{\delta^2 + (A_x/2)^2}$ denotes the Rabi frequency of the Rabi-RWA method. To sum up, the Rabi-RWA Hamiltonian Eq. (A1), which is mathematically simple and analytically solvable, is reduced from the biased Rabi Hamiltonian Eq. (1) after neglecting all the fast oscillatory terms. The CHRW method we develop in this paper is an analytical method that takes into account the effects of the dropped terms and yet preserves the mathematical simplicity of the Rabi-RWA method.

[1] A. J. Leggett, S. Chakravarty, A. T. Dorsey, M. P. A. Fisher, A. Garg, and W. Zwerger, Rev. Mod. Phys. **59**, 1 (1987).

[2] U. Weiss, *Quantum Dissipative Systems*, 3rd ed. (World Scientific, Singapore, 2008).

[3] W. D. Oliver, Y. Yu, J. C. Lee, K. K. Berggren, L. S. Levitov, and T. P. Orlando, Science **310**, 1653 (2005).

[4] R. Hanson and D. D. Awechalom, Nature (London) **453**, 1043 (2008).

[5] X. D. Xu, B. Sun, E. D. Kim, K. Smirl, P. R. Berman, D. G. Steel, A. S. Bracker, D. Gammon, and L. J. Sham, Phys. Rev. Lett. **101**, 227401 (2008).

[6] J. H. Shirley, Phys. Rev. **138**, B979 (1965).

[7] Y. Dakhnovskii and H. Metiu, Phys. Rev. A **48**, 2342 (1993); Y. Dakhnovskii and R. Bavli, Phys. Rev. B **48**, 11020 (1993).

[8] Y. Kayanuma, Phys. Rev. B **47**, 9940 (1993); Phys. Rev. A **50**, 843 (1994).

[9] Y. Kayanuma, Phys. Rev. A **55**, R2495 (1997).

[10] K. Hijii and S. Miyashita, Phys. Rev. A **81**, 013403 (2010).

[11] Ya. S. Greenberg, A. Izmalkov, M. Grajcar, E. Il'ichev, W. Krech, H.-G. Meyer, M. H. S. Amin, and A. Maassen van den Brink, Phys. Rev. B **66**, 214525 (2002); Ya. S. Greenberg, A. Izmalkov, M. Grajcar, E. Il'ichev, W. Krech, and H.-G. Meyer, *ibid.* **66**, 224511 (2002).

[12] Ya. S. Greenberg, Phys. Rev. B **68**, 224517 (2003).

[13] S.-K. Son, S. Han, and Shih-I. Chu, Phys. Rev. A **79**, 032301 (2009).

[14] T.-S. Ho, S.-H. Hung, H.-T. Chen, and Shih-I. Chu, Phys. Rev. B **79**, 235323 (2009).

[15] L. Chotorlishvili, P. Schwaba, Z. Toklikishvili, and V. Skrinnikov, Phys. Lett. A **374**, 1642 (2010); L. Chotorlishvili, Z. Toklikishvili, and J. Berakdar, J. Phys. A: Math. Theor. **44**, 165303 (2011).

[16] Y. Nakamura, Y. A. Pashkin, and J. S. Tsai, Nature (London) **398**, 786 (1999).

[17] E. Il'ichev, N. Oukhanski, A. Izmalkov, Th. Wagner, M. Grajcar, H.-G. Meyer, A. Yu. Smirnov, A. Maassen van den Brink, M. H. S. Amin, and A. M. Zagoskin, Phys. Rev. Lett. **91**, 097906 (2003).

[18] M. S. Rudner, A. V. Shytov, L. S. Levitov, D. M. Berns, W. D. Oliver, S. O. Valenzuela, and T. P. Orlando, Phys. Rev. Lett. **101**, 190502 (2008).

[19] J. Clarke and F. K. Wilhelm, Nature **453**, 1031 (2008).

[20] M. Hofheinz, H. Wang, M. Ansmann, R. C. Bialczak, E. Lucero, M. Neeley, A. D. O'Connell, D. Sank, J. Wenner, J. M. Martinis, and A. N. Cleland, Nature **459**, 546 (2009).

[21] G. Z. Sun, X. D. Wen, B. Mao, Z. Y. Zhou, Y. Yu, P. H. Wu, and S. Y. Han, Phys. Rev. B **82**, 132501 (2010).

[22] J. Berezovsky, M. H. Mikkelsen, N. G. Stoltz, L. A. Coldren, and D. D. Awschalom, Science **320**, 349 (2008).

[23] F. H. L. Koppens, C. Buizert, K. J. Tielrooij, I. T. Vink, K. C. Nowack, T. Meunier, L. P. Kouwenhoven, and L. M. K. Vandersypen, Nature (London) **442**, 766 (2006).

[24] K. C. Nowack, F. H. L. Koppens, Y. V. Nazarov, and L. M. K. Vandersypen, Science **318**, 1430 (2007).

[25] X. D. Xu, B. Sun, P. R. Berman, D. G. Steel, A. S. Bracker, D. Gammon, and L. J. Sham, Science **317**, 929 (2007).

[26] X. D. Xu, B. Sun, P. R. Berman, D. G. Steel, A. S. Bracker, D. Gammon, and L. J. Sham, Nature Phys. **4**, 692 (2008).

[27] T. Hayashi, T. Fujisawa, H. D. Cheong, Y. H. Jeong, and Y. Hirayama, Phys. Rev. Lett. **91**, 226804 (2003).

[28] J. Gorman, D. G. Hasko, and D. A. Williams, Phys. Rev. Lett. **95**, 090502 (2005).

[29] F. Jelezko, T. Gaebel, I. Popa, A. Gruber, and J. Wrachtrup, Phys. Rev. Lett. **92**, 076401 (2004).

[30] G. D. Fuchs, V. V. Dobrovitski, D. M. Toyli, F. J. Heremans, and D. D. Awschalom, Science **326**, 1520 (2009).

[31] B. B. Buckley, G. D. Fuchs, L. C. Bassett, and D. D. Awschalom, Science **330**, 1212 (2010).

[32] M. Grifoni and P. Hänggi, Phys. Rep. **304**, 229 (1998).

[33] S. Ashhab, J. R. Johansson, A. M. Zagoskin, and F. Nori, Phys. Rev. A **75**, 063414 (2007).

[34] F. Bloch and A. Siegert, Phys. Rev. **57**, 522 (1940); D. R. Dion and J. O. Hirschfelder, Adv. Chem. Phys. **35**, 265 (1976); P. K. Aravind and J. O. Hirschfelder, J. Phys. Chem. **88**, 4788 (1984).

[35] J. Tuorila, M. Silveri, M. Sillanpää, E. Thuneberg, Y. Makhlin, and P. Hakonen, Phys. Rev. Lett. **105**, 257003 (2010).

[36] F. Grossmann, T. Dittrich, P. Jung, and P. Hänggi, Phys. Rev. Lett. **67**, 516 (1991).

[37] F. Grossmann and P. Hänggi, Europhys. Lett. **18**, 571 (1992); J. M. Gomez Llorente and J. Plata, Phys. Rev. A **45**, R6958 (1992).

[38] F. Grossmann, T. Dittrich, P. Jung, and P. Hänggi, J. Stat. Phys. **70**, 229 (1993).

[39] J. T. Stockburger, Phys. Rev. E **59**, R4709 (1999).

[40] J. Hausinger and M. Grifoni, Phys. Rev. **A 81**, 022117 (2010).

[41] H. Zheng, S. Y. Zhu, and M. S. Zubairy, Phys. Rev. Lett. **101**, 200404 (2008); Z. H. Li, D. W. Wang, H. Zheng, S. Y. Zhu, and M. S. Zubairy, Phys. Rev. A **80**, 023801 (2009); Q. Ai, Y. Li, H. Zheng, and C. P. Sun, *ibid.* **81**, 042116 (2010).

[42] Z. Ficek, Front. Phys. China **5**, 26 (2010); Z. Ficek and R. Tanaś, Phys. Rep. **372**, 369 (2002); J. Jing, Z. G. Lü, and Z. Ficek, Phys. Rev. A **79**, 044305 (2009).

[43] Y. Y. Yan, Z. G. Lü, and H. Zheng, Phys. Rev. A **88**, 053821 (2013).

[44] F. Yoshihara, Y. Nakamura, F. Yan, S. Gustavsson, J. Bylander, W. D. Oliver, and J. S. Tsai, Phys. Rev. B **89**, 020503(R) (2014).

[45] Z. G. Lü and H. Zheng, Phys. Rev. A **86**, 023831 (2012).

[46] Y. Y. Yan, Z. G. Lü, and H. Zheng, Phys. Rev. A **91**, 053834 (2015).

[47] H. Zheng, Eur. Phys. J. B **38**, 559 (2004); C. Zhao and H. Zheng, Phys. Rev. A **82**, 043844 (2010); Z. G. Lü and H. Zheng, Phys. Rev. B **75**, 054302 (2007); J. Chem. Phys. **131**, 134503 (2009); Europhys. Lett. **86**, 60009 (2009); J. Chem. Phys. **136**, 121103 (2012).

[48] M. O. Scully and M. S. Zubairy, *Quantum Optics* (University Press, Cambridge, 1997).